

## Experimental study of the effect of a supercurrent on high-resistance superconductor–insulator–normal-metal tunnel junctions

Yeouchung Yen,\* Soon-Gul Lee, and Thomas R. Lemberger  
*Department of Physics, Ohio State University, Columbus, Ohio 43210*

(Received 17 April 1987)

We have measured the low-voltage resistance of superconductor–insulator–normal-metal tunnel junctions as a function of supercurrent in the superconducting film. The superconducting films were Sn and Al. The junctions had sufficiently high resistances that nonequilibrium effects associated with a charge imbalance in the superconductor were negligible. We find that the supercurrent reduces the resistance as expected from the dirty-limit theory of superconductivity. We conclude that the theory accurately predicts the pair-breaking effects of supercurrents in films despite inevitable nonuniformities in film thickness and supercurrent density that occur in wide films.

### I. INTRODUCTION

In the course of studying the effect of supercurrents on very low-resistance superconductor–insulator–normal-metal (SIN) tunnel junctions,<sup>1–3</sup> in which nonequilibrium effects are readily measurable, we realized that the effect of supercurrents on high-resistance junctions, in which nonequilibrium effects are negligible, had not been studied carefully. In the present work, we verify that the dirty-limit theory of superconductivity quantitatively describes the reduction that a supercurrent causes in the low-voltage resistance of high-resistance SIN junctions. Results are presented for Sn- and Al-based junctions. Apparently the nonuniform supercurrent density, the variations in film thickness that inevitably exist in thin films, and other imperfections, have a negligible effect on these measurements, even though they reduce the measured critical current substantially.

We follow the dirty-limit theory developed by Maki<sup>4</sup> in our analysis. Maki first calculated the effects on a superconducting film of a transport supercurrent, as well as a current induced with a magnetic field. He showed that the current reduces the order parameter and the transition temperature, and broadens the singularity in the BCS density of states just as magnetic impurities do.<sup>5,6</sup>

Maki's theory assumes that the electron mean free path  $l$  is much less than the pure-limit coherence length  $\xi_0$ . This is true in our Al film, but in the Sn film,  $l \approx \xi_0$ . We use Maki's theory anyway because it is simpler than a general theory and because it describes the data. Maki's theory assumes that the film thickness  $d$  is much less than  $2\lambda(T)$ , where  $\lambda$  is the magnetic penetration depth and the factor of 2 is associated with the top and bottom surfaces of the film. This condition ensures that the current density  $J_s$  for a transport current is uniform through the film thickness, and that  $J_s$  for a parallel magnetic field varies linearly through the film thickness, being zero at the midplane. Our Al film has  $d \ll 2\lambda(T)$

for all  $T$ . Our Sn film has  $d \ll 2\lambda(T)$  near  $T_c$ , but  $d \approx 2\lambda$  at low temperatures. The theory also assumes that  $d$  is much less than twice the Ginzburg-Landau coherence length  $\xi(T)$  so that the order parameter  $\Delta$  is uniform through the thickness. This condition is well satisfied for the Al and Sn films.

The effect of field-induced supercurrents on tunnel junctions was studied by Levine<sup>7,8</sup> and by Millstein and Tinkham.<sup>9</sup> These authors measured the current-voltage characteristics of SIN junctions where supercurrents were induced in the superconducting film by application of a magnetic field parallel to the film's surface. Their results were in good agreement with Maki's theory. More recently, Rasing *et al.*<sup>10</sup> have made similar, high-precision measurements on strong-coupling Pb films and their results are well described by the strong-coupling theory of Daams *et al.*,<sup>11</sup> which is a generalization of Maki's theory. By inducing the supercurrents rather than applying them directly with a current supply, these authors avoided the problem of a nonuniform current density<sup>12</sup> that occurs in films wider than the magnetic penetration depth  $\lambda$ . Furthermore, with a parallel magnetic field it is possible to depress the order parameter continuously to zero. This cannot be done with a transport supercurrent,<sup>13</sup> even in principle, because the superconductor passes into a time-dependent resistive state before the order parameter is depressed to zero.<sup>14</sup>

We are interested in the effects of transport supercurrents, despite the limitations just given, because there are circumstances in which it is very difficult to induce a supercurrent, e.g., in very dirty or thin films. Moreover, in magnetic superconductors the spins would interact with the applied field so that the two methods of inducing a current would likely give different results. Thus, it becomes important to test the validity of the theory of the effect of transport supercurrents in real, typical, films with widths larger than the magnetic penetration depth.

The present work was motivated by these considerations. Paterno *et al.*<sup>15</sup> made similar measurements with a more intricate junction geometry that excluded the

edges of the Sn film, where the current density peaks, from the tunnel junction. Since we find that the edge effects are negligible, our measurements should be viewed as an extension of their work to a wider temperature range and a more rigorous analysis. We focus on the low-voltage resistance, rather than the entire current-voltage characteristic because the low-voltage resistance is most sensitive to supercurrents.

We emphasize that these junctions have sufficiently high resistances that nonequilibrium effects associated with the generation of a quasiparticle charge imbalance by the bias current<sup>16-19</sup> are negligible. We are studying the "equilibrium" component of the junction resistance only.

## II. THEORY

A bias voltage across a SIN tunnel junction results in a current by favoring those random tunneling events in which electrons traverse the insulating barrier to the film with positive bias, or lowered Fermi energy. The normalized low-voltage resistance,  $R_j(T)/R_N$ , has the form<sup>13</sup>

$$R_j(T)/R_N = \left[ 2 \int_0^\infty dE N_1(E) [-\partial f^0(E)/\partial E] \right]^{-1}, \quad (1)$$

where  $N_1(E)$  is the superconducting tunneling density of states normalized to its normal state value and  $f^0(E)$  is the Fermi function.  $R_N$  is the resistance of the junction above the superconducting transition temperature  $T_c$ . [ $R_j(T)$  is essentially the same as  $R_{eq}(T)$  in Ref. 1 since no nonequilibrium effect is involved here.]

In the absence of any pair-breaking mechanism,  $N_1$  assumes the BCS (Ref. 20) form:

$$\begin{aligned} N_1(E) &= 0 \quad \text{for } E < \Delta, \\ &= E / [(E^2 - \Delta^2)]^{1/2} \quad \text{for } E \geq \Delta, \end{aligned} \quad (2)$$

where  $\Delta$  is the order parameter in the superconductor. Results in this limit have been tabulated by Bermon<sup>21</sup> and serve as a check on our computer program. A supercurrent results in a pair-breaking rate:<sup>4</sup>

$$1/\tau_s = D p_s^2 / 2\hbar^2, \quad (3)$$

where  $D = v_f l / 3$  is the electron diffusion constant and  $p_s = 2mv_s$  is the momentum of a Cooper pair of electrons, mass  $m$ , moving with speed,  $v_s$ . Equation (3) is valid in the dirty limit where the electron mean free path  $l$  is much shorter than the pure-limit coherence length  $\xi_0$ . This pair breaker reduces  $\Delta$ , broadens the peak in the density of states, and reduces the density of superconducting electrons  $n_s$ . The change in  $N_1(E)$  results in a reduced junction resistance  $R_j(T, I_s)$  that we observe.

For comparison with experiment, it is useful to express  $1/\tau_s$  in terms of measurable quantities by using free-electron relations among  $D$ , the normal-state density of states  $2N(0)$ , and the resistivity  $\rho$ , and by using dirty-limit expressions for the magnetic penetration depth  $\lambda$  and coherence length  $\xi$ .<sup>13</sup>

$$1/\tau_s = \frac{2\gamma^2 \rho}{\pi^4 2N(0)(k_B T_c)^2 d^2 w^2} \frac{n_s(0,0)^2}{n_s(T, 1/\tau_s)^2} I_s^2. \quad (4)$$

In the derivation of Eq. (4), we have replaced the zero-temperature order parameter  $\Delta(0)$  by its weak-coupling value  $(\pi/\gamma)k_B T_c$  where  $\gamma = 1.7811$ . In this expression,  $d$  and  $w$  are the film thickness and width. Finally, we note that most of the material parameters in Eq. (4) can be absorbed into a single parameter, the critical current at zero temperature  $I_c(0)$  (Ref. 22) so that

$$1/\tau_s = 0.1669 \frac{k_B T_c}{\hbar} \frac{n_s(0,0)^2}{n_s(T, 1/\tau_s)^2} \frac{I_s^2}{I_c(0)^2}, \quad (5)$$

where

$$I_c(0)^2 = \frac{(2.562)2N(0)d^2 w^2 (k_B T_c)^3}{\hbar \rho} \quad (6)$$

Our results below show that the values of  $I_c(0)$  determined by fitting the data for  $R_j(T, I_s)$  versus  $I_s$  are in excellent agreement with values calculated from measured sample parameters and Eq. (6).

In general, numerical calculations are required to obtain  $R_j(T, I_s)$  versus  $I_s$ . Our numerical results were obtained with the same programs described in Ref. 1. Briefly, we calculated  $\Delta(T, 1/\tau_s)$  and  $n_s(T, 1/\tau_s)$  following Maki.<sup>4</sup> Our results reproduced published values for  $\Delta$  (Ref. 4) and for the critical current density (Ref. 22)  $J_c(T)$  obtained from the maximum in current density  $J_s = n_s e v_s$  versus  $1/\tau_s$ . The density of states  $N_1(E)$  was calculated following Beyer-Nielsen.<sup>23,24</sup> In the limit of zero inelastic pair-breaking processes, such as electron-phonon scattering, our results agreed with published results for  $N_1(E)$  in Ref. 24.

The normalized resistance of the junction  $R_j/R_N$  can be calculated by numerical integration of Eq. (1), given the density of states. Figure 1 shows numerical results for  $R_j/R_N$  versus  $I_s^2/I_c(0)^2$ , for several temperatures.  $I_c(0)$  is the theoretical critical current at  $T=0$  for an ideal narrow superconducting film in which the current density is uniform. When the applied pair-breaking rate is small, i.e.,  $\hbar/\tau_s \ll 1$ , the reduction in  $R_j$  is linear in  $1/\tau_s$ , so the reduction is quadratic in  $I_s$ . For large current,  $R_j$  decreases more rapidly because the pair-breaking rate increases more rapidly than current squared. This occurs because the product  $n_s e v_s$  always equals the applied current density, and because the superconducting electron density  $n_s$  decreases as the current increases, forcing the superfluid velocity  $v_s$  to increase faster than linearly with current. The pair-breaking rate is proportional to  $v_s^2$ , so it increases faster than  $I_s^2$  near  $I_c(T)$ . This explains the rapid drop in  $R_j$  as  $I_s$  approaches the critical current  $I_c(T)$  for each curve. The curves do not extend to  $R_j/R_N = 1$  because the critical current is reached before  $\Delta$  is depressed to zero.

Note that the slope of the initial linear depression in  $R_j/R_N$  decreases as  $T$  decreases from  $T_c$ , has a minimum value at  $T/T_c \approx 0.65$ , and finally increases again for lower temperatures. Near  $T_c$ , the different

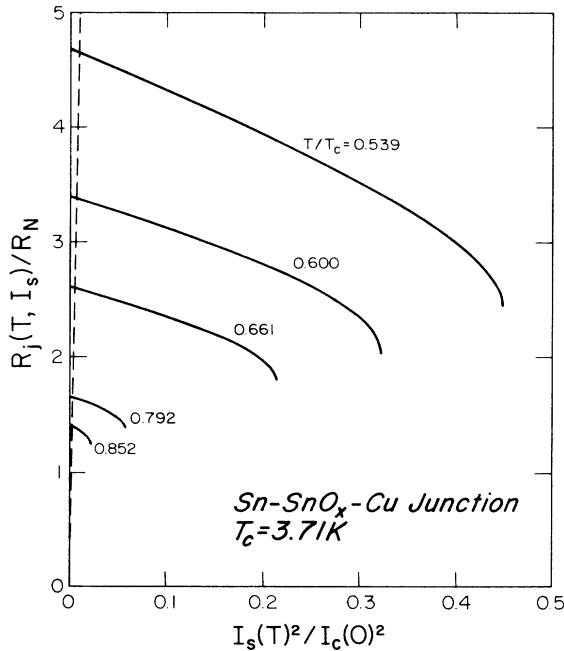


FIG. 1. Calculated normalized low-voltage resistance  $R_j(T, I_s)/R_N$  vs  $I_s(T)^2/I_c(0)^2$  for a SIN junction. The dashed line indicates the experimentally accessible range of super-currents in the present study.

slopes associated with curves for different temperatures reflect the temperature dependence of  $n_s$ . That is, the pair-breaking rate caused by a given current is largest near  $T_c$ , where  $n_s$  is small and  $v_s$  is therefore large. At low temperatures,  $n_s$  is nearly independent of  $T$ , so the pair-breaking rate for a given current is independent of  $T$ . The slope of  $R_j$  versus  $I_s^2$  increases again at low  $T$  because the junction resistance depends exponentially on  $\Delta/k_B T$  at low temperatures. Thus, at low temperatures a given current produces a pair-breaking rate that is independent of  $T$ , and hence a decrease in  $\Delta$  that is independent of  $T$ , but it produces an ever larger decrease in the junction resistance as  $T$  is lowered.

Measured critical currents for wide films are usually smaller than the maximum theoretical values for a uniform current density, presumably due in part to a peak in the current density near the edges of the film.<sup>12</sup> In our films the measured critical currents were only about 20–40% of the theoretical ideal values. Consequently, the maximum pair-breaking rate we obtained experimentally was no more than 5% of the pair-breaking rate at the theoretical maximum value of  $I_c(T)$ . That is, our experimental data stay to the left of the dashed line in Fig. 1.

Finally, note that there are only three parameters for fitting the theory to the data, namely,  $T_c$ ,  $R_N$ , and  $I_c(0)$ .  $T_c$  and  $R_N$  are determined by fitting  $R_j(T)$  near  $T_c$ . The critical current at zero temperature,  $I_c(0)$ , is determined by fitting  $R_j/R_N$  versus  $I_s^2$  at one temperature. As discussed below, fitting at one temperature fits at all

temperatures, and the fitted value of  $I_c(0)$  agrees well with Eq. (6) with measured values of most parameters and the literature value of the density of states  $2N(0)$ , as shown in Table I.

### III. EXPERIMENTAL DETAILS

The samples were Sn-SnO<sub>x</sub>-Cu or Al-AlO<sub>x</sub>-Cu SIN tunnel junctions. All films were deposited from resistively-heated sources through mechanical masks onto glass substrates. To improve the uniformity of the current density, samples were built in substrates with  $\sim(4000-5000)$  Å-thick superconducting Nb ground planes. These ground planes were anodized and then coated with  $\sim 500-2000$  Å of SiO for insulation before use.

Figure 2 depicts the sample geometry and the wiring diagram. The Sn(Al) films were 800 Å (300 Å) thick, the Cu-Al-Fe films were 2000–4000 Å, while the Pb overlayers were 2000 Å. SiO (500–1500 Å thick) was used to define the area of the junctions to an area of  $\sim 300 \mu\text{m} \times 330 \mu\text{m}$ .

The procedures for depositing Sn and Al films were slightly different. Al films were deposited at  $\sim 5$  Å/sec onto room-temperature glass substrates in about  $2 \times 10^{-5}$  Torr O<sub>2</sub> partial pressure to raise the transition temperature to about 1.6 K. The Sn film presented here was pre-deposited at 20–30 Å/sec onto a glass substrate pre-cooled to between  $-65$  and  $-80^\circ\text{C}$  in a  $2 \times 10^{-7}$ -Torr vacuum. It was found that this substrate temperature range yielded the highest quality Sn films. The substrate was warmed up to room temperature before the Sn film was oxidized with an oxygen glow discharge. Thermal oxidation in a few Torr pressure of O<sub>2</sub> was used for Al films.

After oxidizing the base film, the area of the junctions was defined by depositing SiO to mask off all but 300  $\mu\text{m}$  in length of the narrow part of the base films. The substrate was then cooled to about  $-10$  to  $-20^\circ\text{C}$  before counter-electrode deposition. A mixture of Cu, Al, (3 wt. %), and Fe (3 wt. %) was evaporated in a  $2 \times 10^{-4}$  torr O<sub>2</sub> partial pressure to completion to finish the tunnel junctions. The addition of Al and Fe, as well as evaporation in an oxygen atmosphere, shortened the electron mean free path in the Cu, and prevented any superconducting order induced in the Cu by the Pb overlayer from reaching the junction. It was essential to keep the substrate cold during Cu deposition to avoid wetting of Cu by Sn. The Pb overlayer was deposited to reduce the series resistance of the normal metal strip in the superconducting quantum interference device (SQUID) voltmeter loop. The samples were finished by being covered with  $\sim 200$  Å SiO to protect films from recrystallization from moisture in the air.

For the Al film,  $l/\xi_0 \approx 2.9 \text{ nm}/1600 \text{ nm} \ll 1$ , and for the Sn film,  $l/\xi_0 \approx 141 \text{ nm}/230 \text{ nm} \approx 0.6$ . Thus, the Al film is in the extreme dirty limit but the Sn film is not. For the Al film,

$$2\lambda(0)/d \approx 2\lambda_L(0)(1 + \xi_0/l)^{1/2}/d \approx 750 \text{ nm}/30 \text{ nm} \gg 1, \text{ and for the Sn film, } 2\lambda(0)/d \approx 86 \text{ nm}/80 \text{ nm} \approx 1. \text{ There-}$$

TABLE I. Sample and material parameters.

S film material	$T_c$ (K)	$\rho_{4.2}$ (n $\Omega$ m)	$l^a$ (nm)	$w$ ( $\mu$ m)	$d^b$ (nm)	$R_N$ (m $\Omega$ )	$I_c(0)$ (A)	$I_c(0)^{\text{theor}}$ (A)
Al	1.683	138	2.9	315	30	270	0.259	0.207
Sn	3.710	7.45	141	313	80	12.5	6.47	6.90

<sup>a</sup>Determined by using  $\rho_{4.2}l = 1.05 \times 10^{-15}$  and  $4.0 \times 10^{-16}$   $\Omega$  m<sup>2</sup> for Sn (Ref. 12) and Al (Ref. 22), respectively.

<sup>b</sup>Reading obtained from a crystal thickness monitor. This is the thickness used in calculating  $I_c(0)^{\text{theor}}$ .

fore, the current density  $J_s$  in the Al film should be uniform through the film thickness, but  $J_s$  varies slightly in the Sn film, at least at low temperatures. This variation is probably negligible since, for small variations, we expect that the average value of  $J_s^2$  is very close to the spatial average of  $J_s$ , squared, so that it is correct to calculate the current-induced pair-breaking rate from the average current density, which is the total current divided by the crosssectional area of the film. For the Al and Sn films,  $d/2\xi \approx d/2\sqrt{\xi_0}l \ll 1$ , so the order parameter should be uniform through the film thickness.

For the Sn sample we connected a manganin wire of about  $0.2\Omega$  in parallel with the Sn film. This was necessary to avoid excess heating in the Sn film when the critical current was exceeded. This additional wire, however, did not affect our measurements since the Sn film was in the superconducting state.

All junction resistance measurements were done with an rf SQUID in a feedback nulling mode. Typical volt-

age resolution was about 10 pV in a 10 Hz bandwidth. The bias voltage across the tunnel junction was kept smaller than 10  $\mu$ V so that the  $I$ - $V$  characteristic was linear and heating in the junction was not important. In our supercurrent effect measurements the junction bias current was kept fixed and the reduction in the junction voltage was measured. In the absence of a junction bias current, within experimental error, no voltage was observed for current  $I_s$  up to the experimentally accessible critical current, demonstrating that the Al and Sn films were superconducting at currents where  $R_j(T, I_s)$  was measured.

#### IV. EXPERIMENTAL RESULTS AND DISCUSSION

Table I lists the relevant sample and material parameters.  $T_c$  is the transition temperature,  $d$  and  $w$  are the thickness and width of the film,  $\rho_{4.2}$  is the resistivity of the superconducting films at 4.2 K, and  $l$  is the electron mean free path, determined by using  $\rho_{4.2}l = 1.05 \times 10^{-15}$  and  $4.0 \times 10^{-16}$   $\Omega$  m<sup>2</sup> for Sn (Ref. 12) and Al (Ref. 22) respectively.  $R_N$  is the resistance of the junction at  $T_c$ .  $T_c$  and  $R_N$  were chosen to give a best fit to  $R_j(T)$  versus  $T$  near  $T_c$ .  $I_c(0)$  was determined from the best fit to  $R_j(T, I_s)/R_j(T, I_s=0)$  versus  $I_s(T)^2/I_c(0)^2$ .  $I_c(0)^{\text{th}}$  was calculated from Eq. (6) with  $2N(0) = 2.78 \times 10^{28}$  and  $3.48 \times 10^{28}$  eV<sup>-1</sup> m<sup>-3</sup> for Sn and Al, respectively.<sup>25</sup> The values of  $\rho$  for the Al samples are uncertain to about 30% because of a wiring problem.

Figure 3 shows the low-voltage resistance  $R_j(T)/R_N$  versus  $T/T_c$  for the two samples discussed here, together with the calculated curve. Near  $T_c$ ,  $R_j(T)$  is only linear in  $T$  because  $k_B T$  is comparable to or larger than  $\Delta$ , so the gap in the density of states blocks the tunneling of relatively few quasiparticles. At low temperatures, however, the resistance rises exponentially as the number of quasiparticles sufficiently energetic to tunnel into the superconductor vanishes exponentially.

Figure 3 shows that the junctions reported here have slightly larger resistances at low temperature than predicted by BCS theory. The difference can be explained by an enhancement of  $\Delta$  of about 10% due to strong electron-phonon coupling. Strong coupling is not included in the analysis of  $R_j(T, I_s)$  versus  $I_s$ .

Figures 4(a) and 4(b) show the reduction in junction resistance normalized to the junction resistance at zero supercurrent,  $-\delta R_j(T, I_s)/R_j(T, I_s=0)$ , as a function of normalized supercurrent squared,  $I_s(T)^2/I_c(0)^2$ . The solid lines are calculated as outlined above. The temper-

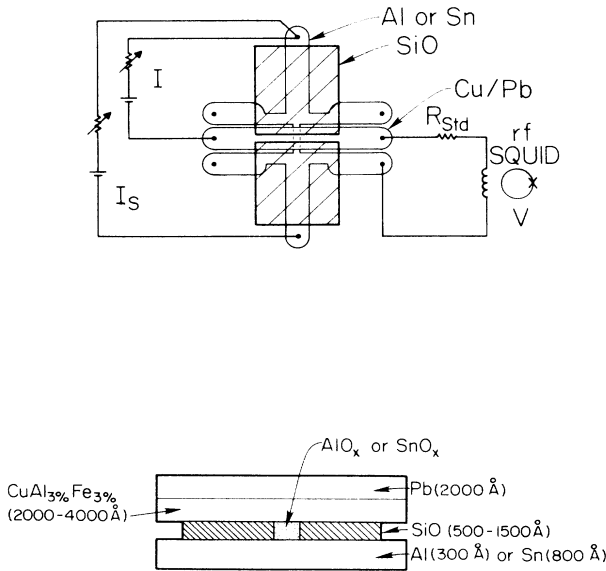


FIG. 2. Sample configuration: plan (top); side (bottom).  $I$  and  $V$  are the current and voltage in the junction;  $I_s$  is the supercurrent in the superconducting strip. For simplicity, the Nb ground plane is not shown here.  $R_{\text{std}}$  is a “standard” resistor. For the Sn sample a  $\sim 0.2\Omega$  wire was connected in parallel with the narrow part of the  $S$  film so that most current flows through the  $0.2\Omega$  short when the critical current is exceeded.

ature dependence of the data is in excellent agreement with theory over the entire temperature range from  $0.33T_c$  to  $0.97T_c$ . Note that although the percentage changes in the junction resistance with supercurrent are all about the same, the change  $\delta R_j$  varies by a factor of 100 between  $0.85$  and  $0.33T_c$ .

The  $\delta R_j(T, I_s)$  versus  $I_s$  curves we measured were usually symmetric with respect to the  $I_s = 0$  point. The current bias through the junction was negligible compared to the applied supercurrent. However, the point of symmetry occasionally shifted to a different value which was larger than half of the bias current through the junction. We showed data for which supercurrent was measured with respect to the symmetry point. The uncertainty created in doing this is no more than 5%.

As shown in Table I, the value of  $I_c(0)$  that gave the best fit to the Sn data was within 10% of the value calculated from the measured properties of the sample and the density of states from the literature. The value used for Al was also in good agreement with the calculated value, given the relatively large uncertainty in  $\rho$ . We conclude that the dirty-limit theory gives an excellent description of the pair-breaking effect of an applied supercurrent on the low-voltage resistance of high-resistance SIN tunnel junctions even in wide films in which the current density is not uniform.

We would expect this result to break down for films with widths  $w$  a little larger than the transverse penetration depth  $\lambda_{\perp} \equiv \lambda^2/d$ . For  $w \gg \lambda_{\perp}$ , as in the present measurements,  $J_s$  is uniform over almost the entire

width of the film and is very nearly equal to the total current divided by the cross-sectional area of the film.  $J_s$  peaks only near the edges, so that the pair-breaking rate is the same over most of the film. For  $w \ll \lambda_{\perp}$ ,  $J_s$  is uni-

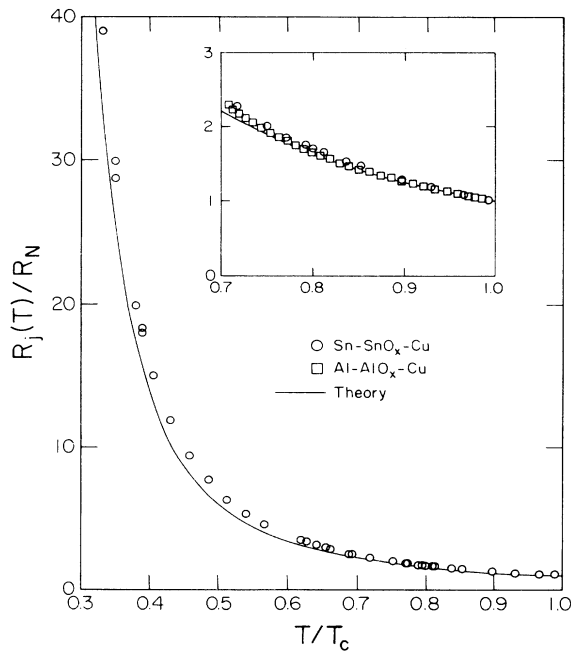


FIG. 3. Experimental values of the normalized low-voltage resistance  $R_j/R_N$  as a function of temperature together with the calculated curve. The slightly larger resistance measured at low temperatures can be explained by an enhancement of  $\Delta$  of about 10% due to strong electron-phonon coupling.

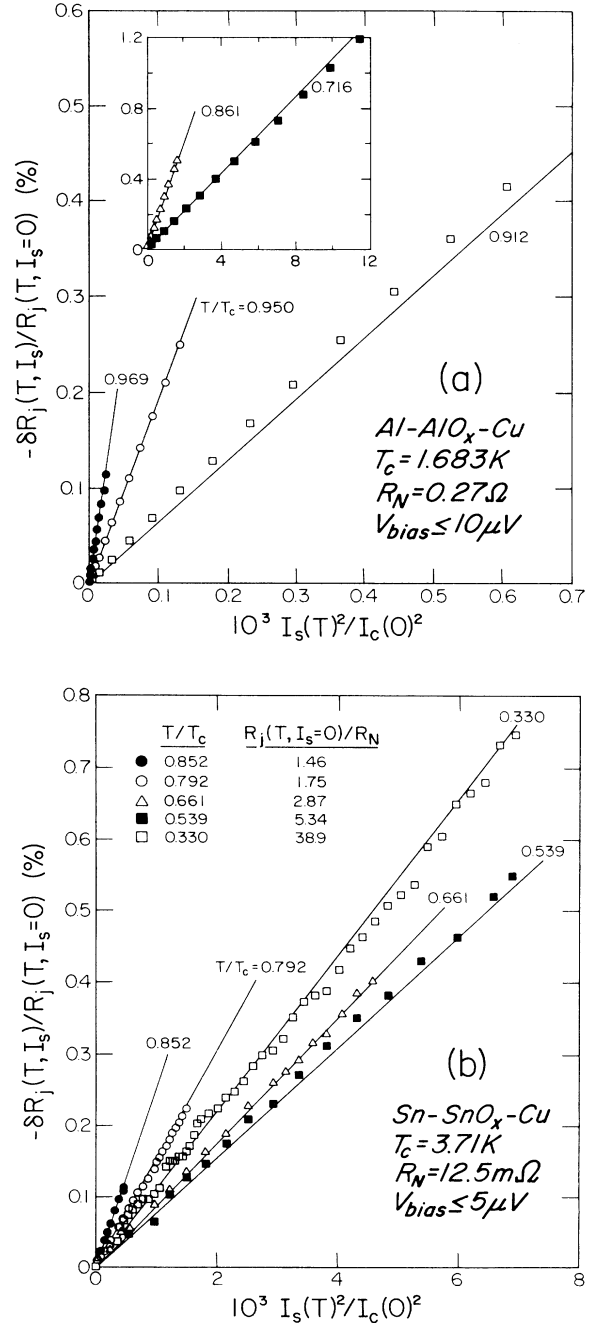


FIG. 4. Reduction in junction resistance normalized to the junction resistance at zero supercurrent,  $-\delta R_j(T, I_s)/R_j(T, I_s=0)$ , as a function of normalized supercurrent squared,  $I_s(T)^2/I_c(0)^2$ , for (a) Al-AlO<sub>x</sub>-Cu and (b) Sn-SnO<sub>x</sub>-Cu junctions. The solid lines are the theoretical results. The temperature dependence of the data is in excellent agreement with theory over the entire temperature range from  $0.33T_c$  to  $0.97T_c$ .

form across the entire film. It is only for  $w$  comparable to  $\lambda_{\perp}$  that large areas of the film have significantly different values of  $J_s$ , and hence different pair-breaking rates.

## V. CONCLUSION

We have studied the reduction in the low-voltage resistance of high-resistance superconductor–insulator–normal-metal tunnel junctions by an applied supercurrent. The data on Sn- and Al-based junctions are in excellent qualitative and quantitative agreement with the dirty-limit theory over the entire temperature range studied,  $0.33 < T/T_c < 0.97$ . We conclude that nonuniformities in the current density and film thickness, which limit the measured critical current below the theoretical maximum, do not have a significant effect on the average

pair-breaking effect of a transport supercurrent. Similar measurements may be useful in studying novel superconducting materials.

It would be interesting to extend this study to thick films in which the current density varies significantly through the film thickness, to cleaner films to see where the dirty-limit theory becomes inapplicable, and to narrower films to study the effect of peaks in the current density at the edges of the film.

## ACKNOWLEDGMENTS

This material is based upon work supported by the National Science Foundation under Grants Nos. DMR-83-00254 and DMR-85-15370. This work was also supported by a Joseph H. Defrees Grant from the Research Corporation. One of us (T.R.L.) wishes to acknowledge support from the Alfred P. Sloan Foundation.

---

\*Present address: INTEL Corporation, Portland, OR 97219.

<sup>1</sup>T. R. Lemberger, Y. Yen, and S. G. Lee, *Phys. Rev. B* **35**, 6670 (1987).

<sup>2</sup>Y. Yen and T. R. Lemberger (unpublished).

<sup>3</sup>S. G. Lee and T. R. Lemberger (unpublished).

<sup>4</sup>K. Maki, in *Superconductivity*, edited by R. D. Parks (Dekker, New York, 1969), p. 1037.

<sup>5</sup>A. A. Abrikosov and L. P. Gor'kov, *Zh. Eksp. Teor. Fiz.* **39**, 1781 (1960) [*Sov. Phys.—JETP* **12**, 1243 (1961)].

<sup>6</sup>S. Skalski, O. Betbeder-Matibet, and P. R. Weiss, *Phys. Rev.* **136**, A1500 (1964).

<sup>7</sup>J. L. Levine, *Phys. Rev.* **155**, 373 (1967).

<sup>8</sup>J. L. Levine, *Phys. Rev. Lett.* **15**, 154 (1965).

<sup>9</sup>J. Millstein and M. Tinkham, *Phys. Rev.* **158**, 325 (1967).

<sup>10</sup>Th. H. M. Rasing, H. W. M. Salemink, P. Wyder, and S. Strässler, *Phys. Rev. B* **23**, 4470 (1981).

<sup>11</sup>J. M. Daams, H. G. Zarate, and J. P. Carbotte, *Phys. Rev. B* **30**, 2577 (1984).

<sup>12</sup>W. J. Skocpol, *Phys. Rev. B* **14**, 1045 (1976).

<sup>13</sup>See, for example, M. Tinkham, *Introduction to Superconductivity* (McGraw-Hill, New York, 1975), p. 117.

<sup>14</sup>L. G. Aslamazov and S. V. Lennitskii, *Zh. Eksp. Teor. Fiz.*

**84**, 2216 (1983) [*Sov. Phys.—JETP* **57**, 1291 (1983)].

<sup>15</sup>G. Paterno, M. V. Ricci, and N. Sacchetti, *Phys. Rev. B* **3**, 3792 (1971).

<sup>16</sup>T. R. Lemberger, *Phys. Rev. Lett.* **52**, 1029 (1984).

<sup>17</sup>T. R. Lemberger, *Phys. Rev. B* **29**, 4946 (1984).

<sup>18</sup>T. R. Lemberger and Y. Yen, *Phys. Rev. B* **29**, 6384 (1984).

<sup>19</sup>Y. Yen and T. R. Lemberger, *Proceedings of the 17th International Conference on Low-Temperature Physics, LT-17*, edited by U. Eckern, A. Schmid, W. Weber, and H. Wühl (North Holland, Amsterdam, 1984), p. 429.

<sup>20</sup>J. Bardeen, L. N. Cooper, and J. R. Schrieffer, *Phys. Rev.* **108**, 1175 (1957).

<sup>21</sup>S. Bermon, Technical Report No. 1, University of Illinois, Urbana Ill., 1964 (unpublished).

<sup>22</sup>J. Romijn, T. M. Klapwijk, M. J. Renne, and J. E. Mooij, *Phys. Rev. B* **26**, 3648 (1982).

<sup>23</sup>J. Beyer-Nielsen, Ph.D. thesis, H. C. Oersted Institute, 1983 (unpublished).

<sup>24</sup>J. Beyer-Nielsen, J. Rammer, H. Smith, and C. J. Pethick, *J. Low Temp. Phys.* **46**, 565 (1982).

<sup>25</sup>C. Kittel, *Introduction to Solid State Physics*, 5th ed. (Wiley, New York, 1976).